Pressure effect on the charge density wave instabilities in the quasi-two-dimensional conductors $(PO_2)_4(WO_3)_{2m}$ (m = 4, 5, 6) and η-Mo_4O_{11}

2001 J. Phys.: Condens. Matter 13 1517

(http://iopscience.iop.org/0953-8984/13/7/313)

INSTITUTE OF PHYSICS PUBLISHING JOURNAL OF PHYSICS: CONDENSED MATTER

J. Phys.: Condens. Matter **13** (2001) 1517–1527 www.iop.org/Journals/cm PII: S0953-8984(01)18266-4

Pressure effect on the charge density wave instabilities in the quasi-two-dimensional conductors $(PO_2)_4(WO_3)_{2m}$ (m = 4, 5, 6) and η-Mo_4O_{11}

J Beille[1], U Beierlein[2], J Dumas[2], C Schlenker[2] and D Groult[3]

[1] Laboratoire L Néel, CNRS, BP 188, 38042 Grenoble Cedex 9, France
[2] Laboratoire d'Etudes des Propriétés Electroniques des Solides, CNRS, BP 188, 38042 Grenoble Cedex 9, France
[3] Laboratoire CRISMAT, ISMRA, 6 Boulevard Maréchal Juin, 14050 Caen Cedex, France

Received 18th October 2000, in final form 7 December 2000

Abstract

We report a comparative study of the electrical resistivity under hydrostatic pressure up to 18 kbar of the quasi-two-dimensional conductors $(PO_2)_4(WO_3)_{2m}$ ($m = 4, 5, 6$) and η-Mo_4O_{11}, which show Peierls transitions towards a charge density wave state. The pressure dependences of the transition temperatures are discussed in relation with the hidden nesting properties of these oxides. The results for η-Mo_4O_{11} are compared with previous works.

1. Introduction

Low dimensional metallic oxides show two types of electronic instability, either a Peierls type transition towards a charge density wave (CDW) state or a superconducting instability. The existence of Peierls transitions is associated with Fermi surfaces (FS) showing nesting properties in the normal state. These latter instabilities give rise to gap openings on the FS and to metal–semiconductor transitions in the one dimensional (1D) case or to metal–metal transitions in the quasi-two-dimensional (2D) case where electron and hole pockets are left on the FS in the CDW state. This is the case of the quasi-two-dimensional monophosphate tungsten bronzes with the general formula $(PO_2)_4(WO_3)_{2m}$, where m is an integer which can be varied from 4 to 14 [1, 2] and of the Magneli phase η-Mo_4O_{11} [3–6], which shows a crystal structure similar to that of the compound with $m = 6$. All these oxides have partially filled bands and several electron and hole Fermi surfaces. The lattice of $(PO_2)_4(WO_3)_{2m}$ is orthorhombic with pentagonal tunnels. It consists of ReO_3-type infinite layers of WO_6 octahedra parallel to the (a, b) plane, separated by layers of PO_4 tetrahedra. Since the 5d conduction electrons are mainly confined in the centre of the WO_6 octahedra, the electronic properties are quasi-2D. Their FS has been described in terms of a superposition of hidden one dimensional surfaces associated with infinite chains of WO_6 octahedra along the a, $(a + b)$

and $(a - b)$ directions, which correspond to parallel planes on the FS [7]. This is the so-called hidden nesting or hidden one dimensionality. All these oxides exhibit CDW instabilites [8–10]. The compound with $m = 5$ exists under two different varieties: the crystal structure of the first type is built up of a regular stacking of layers corresponding to $m = 5$. It shows two Peierls transitions [11]. For the second type, the crystal structure is made of layers of WO_6 octahedra of different thicknesses. The structure can be viewed as a regular intergrowth of slabs with $m = 4$ and $m = 6$. This alternate structure is more stable than the first one. X-ray studies of this alternate structure have revealed one Peierls transition accompanied by a non-monotonic thermal variation of the satellite intensity [12] while resistivity measurements show two anomalies [13].

In the $(PO_2)_4(WO_3)_{2m}$ bronzes, the low dimensional character and the average conduction electron density can be varied with the parameter m. The number of conduction electrons per primitive cell is always 4, independent of m. The average number of conduction electrons per W is $2/m$, decreasing with m. The thickness of the perovskite $[WO_3]$-type slabs and therefore the c parameter are increasing with m, while a and b weakly depend on it. The Peierls temperatures increase with m [1, 2].

A renewed interest in η-Mo_4O_{11} has been generated after the discovery of a quantum-Hall-effect-like behaviour [14]. The crystal structure of η-Mo_4O_{11} is built with infinite layers of MoO_6 octahedra separated by MoO_4 tetrahedra. The 4d conduction electrons are confined in the MoO_6 layers. η-Mo_4O_{11} shows two CDW transitions [3–6].The model of hidden nesting is also valid for this oxide.

Pressure studies may give valuable information to improve the understanding of the CDW instabilities in these low dimensional conductors. We have reported earlier the effect of an hydrostatic pressure on the quasi-2D CDW oxide $K_{0.9}Mo_6O_{17}$ [15]: T_p decreases at low pressure ($p < 6$ kbar) then increases at higher pressure. In the case of $Na_{0.9}Mo_6O_{17}$, T_p increases monotonically with pressure [16]. In $Li_{0.9}Mo_6O_{17}$, an increase of the superconducting transition temperature is associated with a decrease of the temperature of the electronic instability [17]. Pressure studies performed on η-Mo_4O_{11} up to 12 kbar [5, 6] have shown that T_{p1} increases with pressure while T_c decreases (table 1).

In this article, we report studies of the effect of a hydrostatic pressure on the resistivity of the monophosphate tungsten bronzes with $m = 4$, $m = 6$ and $m = 5$ with alternative structure as well as of η-Mo_4O_{11} up to 18 kbar. The pressure dependences of the transition temperatures are discussed in relation with the hidden nesting properties. The results for η-Mo_4O_{11} are compared with previous works.

Table 1. Wavevector of the CDW modulation; pressure dependence of the transition temperatures.

Compound	Wavevector of the modulation (reciprocal lattice units)	dT_{p1}/dP (K kbar^{-1})	dT_{p2}/dP or dT_c/dP (K kbar^{-1})
$m = 4$	$T_{p1} = 80$ K: $q_1 = (0.330; 0.295; 0)$	-3.6	$+0.9$ ($P < 5$ kbar)
	$T_{p2} = 52$ K: $q_2 = (0.340; 0; ?)$ [10]		-2.8 ($P > 5$ kbar)
$m = 5$	$T_{p1} = 158$ K: $q_1 = (0.330; 0.330; 0)$	-3.5	$+0.3$
(alternative structure)	$T_c = 30$ K [12, 13]		
$m = 6$	$T_{p1} = 120$ K: $q_1 = (0.385; 0; 0)$	-0.9	-5
	$T_{p2} = 62$ K: $q_2 = (0.310; 0.295; ?)$ [10]		
η-Mo_4O_{11}	$T_{p1} = 109$ K: $q_1 = (0; 0.23; 0)$ [3]	+0.6 (this work)	-1.3 ($P > 13$ kbar; this work)
	$T_c = 30$ K	+1 [5]	-1 [5]

2. Experimental details

The monophosphate tungsten bronzes $(PO_2)_4(WO_3)_{2m}$ with $m = 4, 5, 6$ were prepared using the chemical vapour transport technique [18]. The crystals are platelets parallel to the (a, b) conducting plane with typical size $1.5 \times 0.5 \times 0.2$ mm^3. η-Mo_4O_{11} crystals were also prepared by the chemical vapour technique [3]. In this case, the platelets are parallel to the (b, c) conducting plane with a size similar to that of the monophoshate bronzes. The crystals were first washed in ammonia, then four silver pads were evaporated onto the surface of the sample. Gold wires were attached onto the contact pads with silver epoxy. Contact resistances were a few ohms, three orders of magnitude larger than the resistance measured at 4.2 K. The resistivity measurements were performed with the dc current applied parallel to the (a, b) plane in the case of the monophosphate bronzes and in the (a, c) conducting plane in the case of η-Mo_4O_{11}. Hydrostatic pressure, up to 18 kbar, was generated in a beryllium–copper self-clamped vessel. The sample was pressurized inside a Teflon capsule by a 50:50 pentane:isoamyl alcohol mixture. The pressure is in all cases applied at room temperature and the resistivity curves are recorded upon cooling. The reproducibility of the data was checked for each set of measurements, thus indicating that the sample did not degrade upon pressure or thermal cycling. The transition temperatures are obtained from the minimum in the plot of the derivative $d\rho/dT$ as a function of temperature.

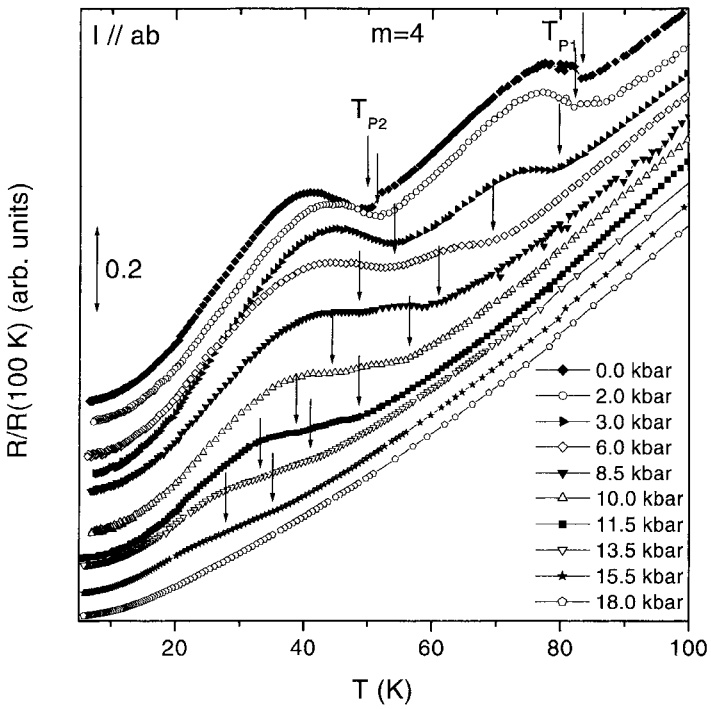

Figure 1. Temperature dependence of the in-plane resistivity normalized at 100 K at various pressures for an $m = 4$ crystal. Curves are shifted for clarity.

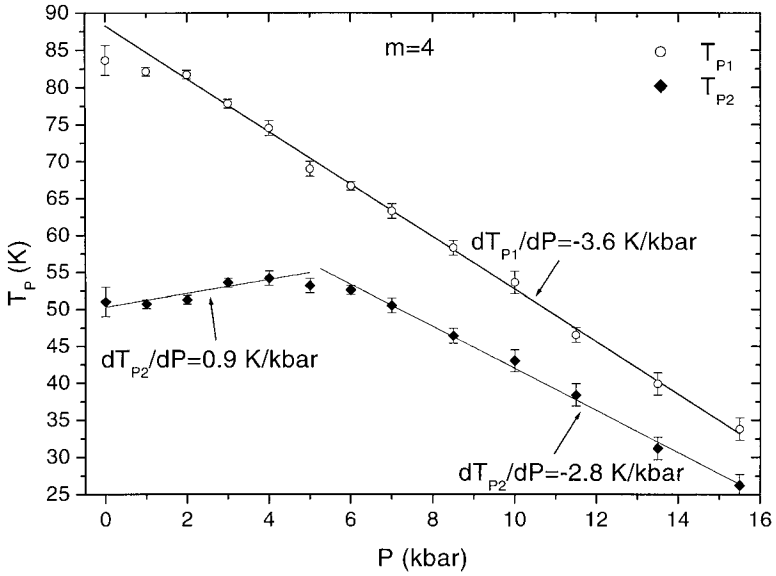

Figure 2. Transition temperatures T_{p1} and T_{p2} as a function of pressure for an $m = 4$ bronze.

3. Experimental results

Figure 1 shows the curves of the resistivity versus temperature at different pressures for an $m = 4$ crystal. At ambient pressure, the two transitions at $T_{p1} = 80$ K and $T_{p2} = 52$ K are clearly visible. A metallic behaviour is observed. The opening of Peierls gaps at T_{p1} and T_{p2} gives rise to an increase in resistivity. Below T_{p2}, the metallic behaviour is restored due to the remaining charge carriers on the Fermi surface. At low pressures, $P < 5$ kbar, T_{p2} increases slightly, then above 5 kbar T_{p2} decreases linearly with pressure. T_{p1} decreases linearly with pressure in the whole range of pressure investigated. The transition becomes broader and broader as the pressure is increased. The broadening of the transitions cannot be due to cracks in the crystal since the resistivity curves are reproducible. Above approximately 15.5 kbar, the Peierls distortions disappear. The pressure dependences of T_{p1} and T_{p2} as reported in figure 2 and the rates $\mathrm{d}T_{p1}/\mathrm{d}P$ and $\mathrm{d}T_{p2}/\mathrm{d}P$ are given in table 1, which summarizes all the results together with the wavevectors of the CDW modulations. One should note that the rate of decrease of T_{p1} is comparable to that found in the quasi-1D compound $NbSe_3$ [19].

Figure 3 shows the curves of the resistivity versus temperature at different pressures for an $m = 6$ compound. The transition temperature T_{p1} decreases slowly with pressure while T_{p2} decreases more rapidly. Above 10 kbar, the transition at T_{p2} vanishes. Figure 4 shows the pressure dependences of T_{p1} and T_{p2}.

Figures 5(a) and (b) show the resistivity curves for an $m = 5$ compound with alternate $4/6/4/6$ structure. T_{p1}, corresponding to a shallow minimum in the resistivity curve, decreases with pressure at the same rate as that of the $m = 4$ compound. Above 18 kbar, the transitions are barely visible. However, in contrast to the $m = 4$ and $m = 6$ compounds, T_c, corresponding to a kink in the resistivity curve, increases slowly as the pressure is increased. Figures 6(a) and (b) summarize the transition temperatures T_{p1} and T_c as a function of pressure for the $m = 4/6$ compounds.

Figure 7 shows the resistivity curves as a function of temperature for different pressures for an η-Mo_4O_{11} crystal. The transition temperature T_{p1} increases linearly with pressure with

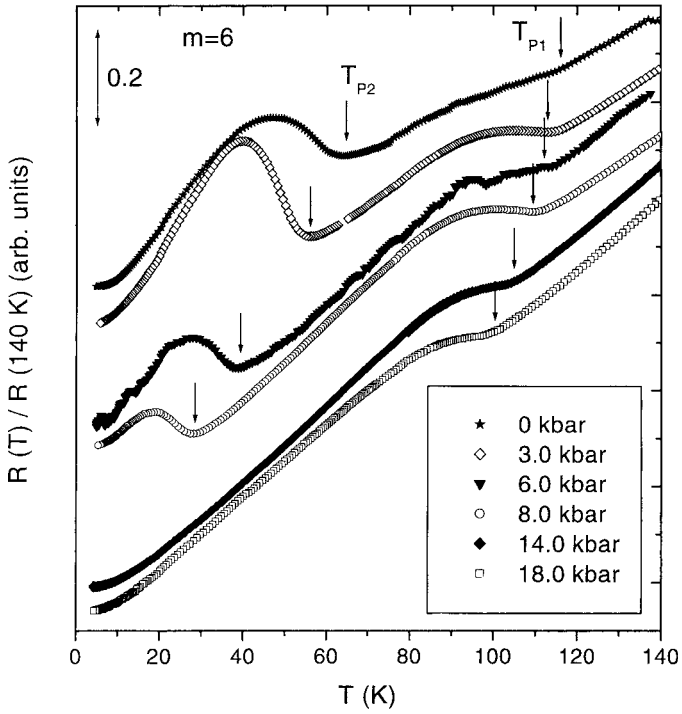

Figure 3. Temperature dependence of the in-plane resistivity normalized at 140 K at various pressures for an $m = 6$ crystal. Curves are shifted for clarity.

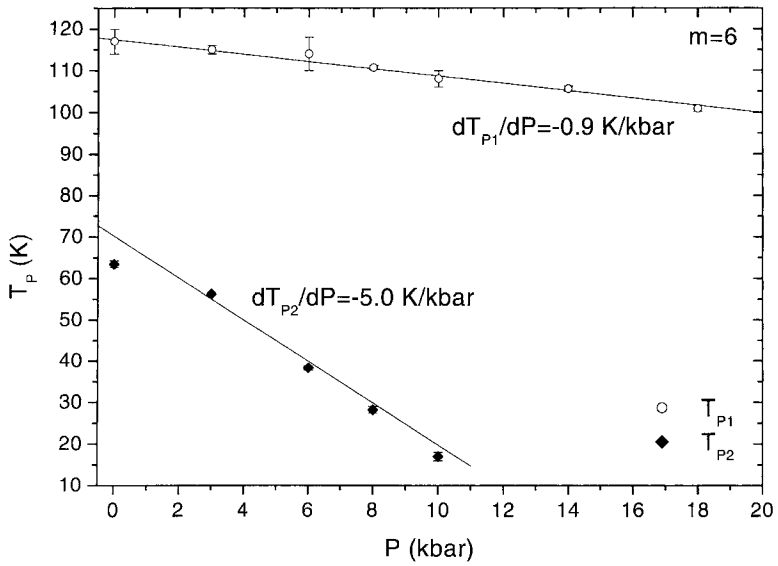

Figure 4. Transition temperatures T_{p1} and T_{p2} as a function of pressure for an $m = 6$ crystal.

a rate somewhat smaller than the value reported in [5]. The behaviour of the anomaly at T_c is more complex. While the amplitude of the anomaly at T_{p1} decreases under pressure, the

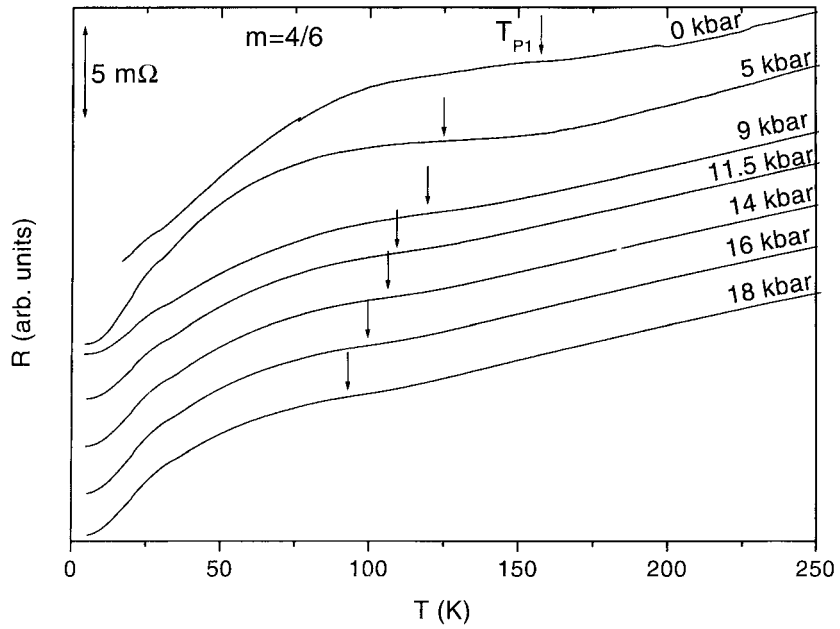

(a)

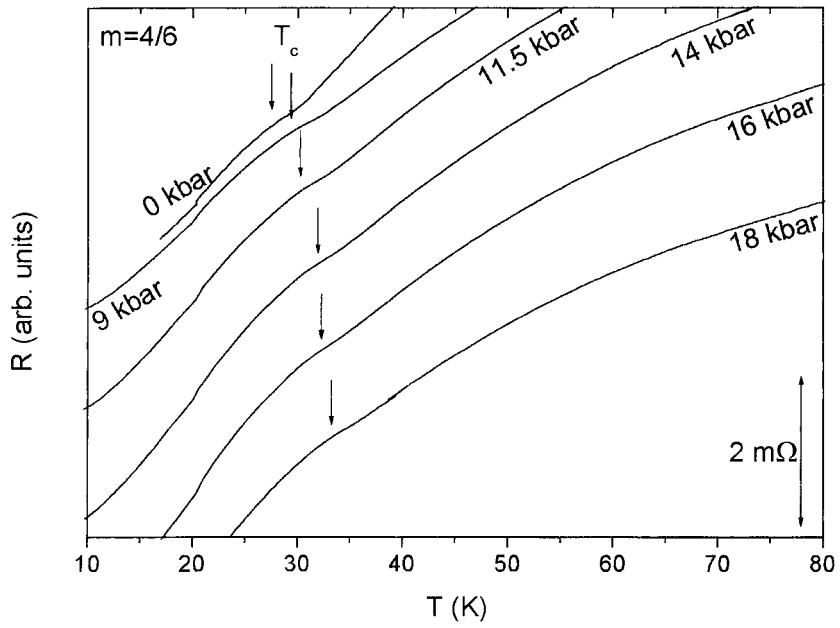

(b)

Figure 5. (a) Temperature dependence of the in-plane resistance at various pressures for an $m = 4/6$ crystal. Curves are shifted for clarity. (b) The same as in figure 5(a) for the temperature range 10–80 K.

amplitude of the anomaly at T_c seems to be enhanced for $P < 10$ kbar. For $P < 13$ kbar, T_c seems to increase slightly with pressure and, above 13 kbar, T_c clearly decreases. Figure 8

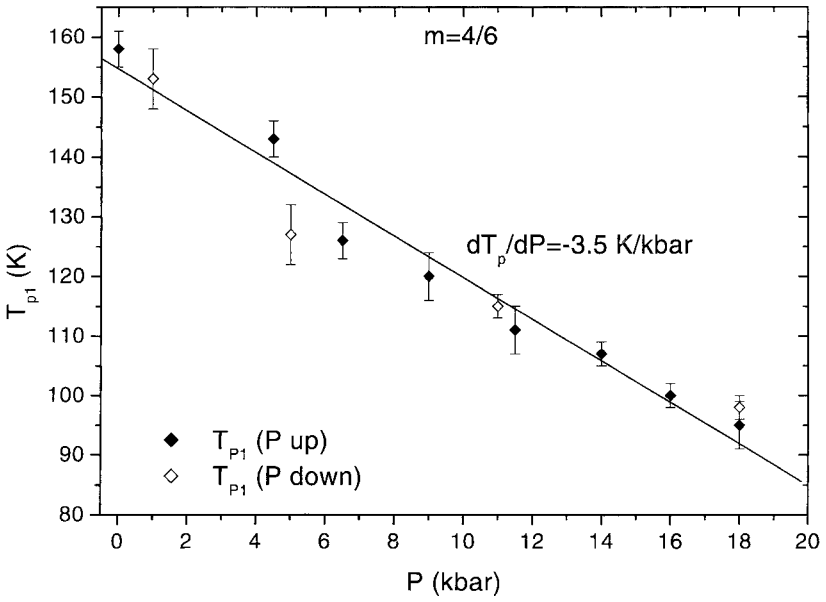

(a)

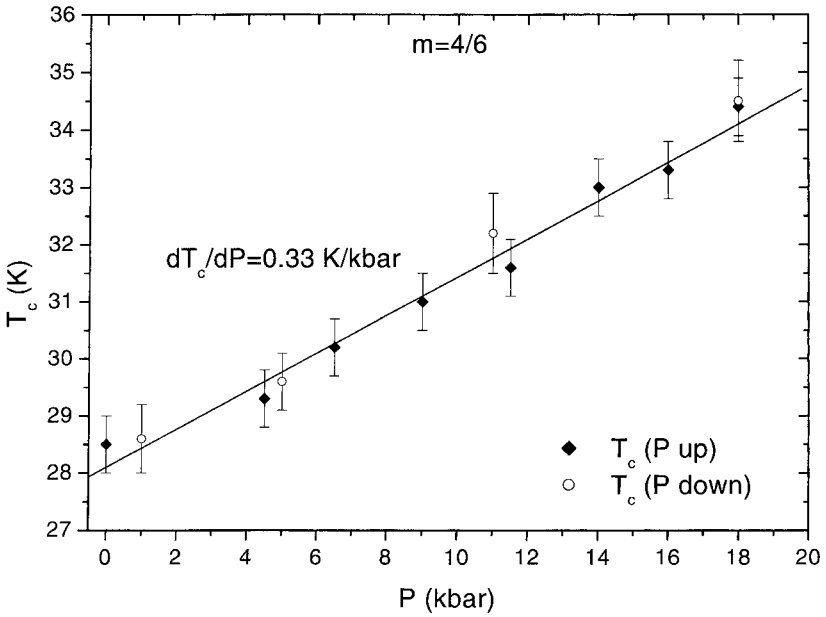

(b)

Figure 6. (a) Transition temperature T_{p1} as a function of pressure for $m = 4/6$. (b) Transition temperature T_c as a function of pressure for $m = 4/6$.

shows the pressure dependence of T_{p1} and T_c. For $P > 13$ kbar, a remarkable feature is the rise of the resistivity below T_c upon cooling. For $P = 15.4$ kbar and 18 kbar, the resistivity shows a plateau at low temperature.

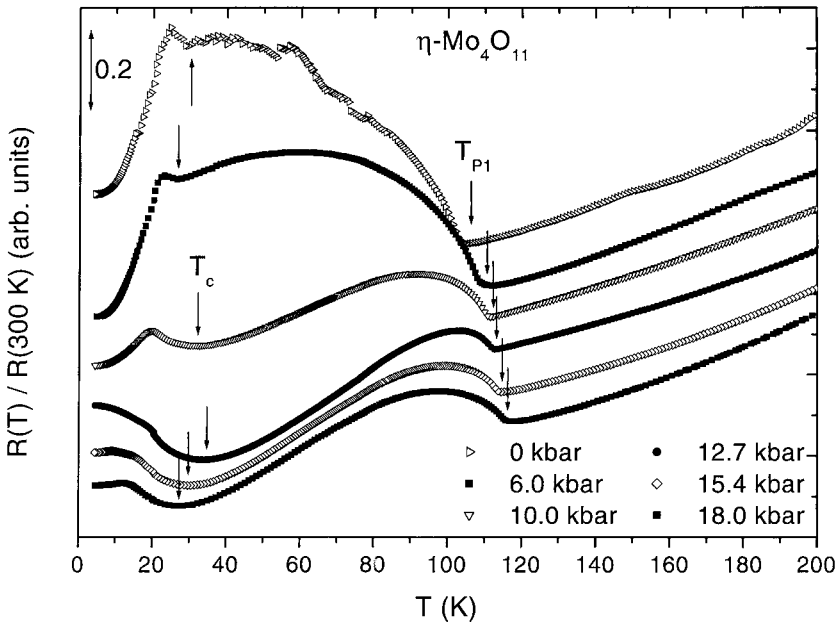

Figure 7. Temperature dependence of the in-plane resistivity at various pressures for an η-Mo_4O_{11} crystal. Curves are shifted for clarity.

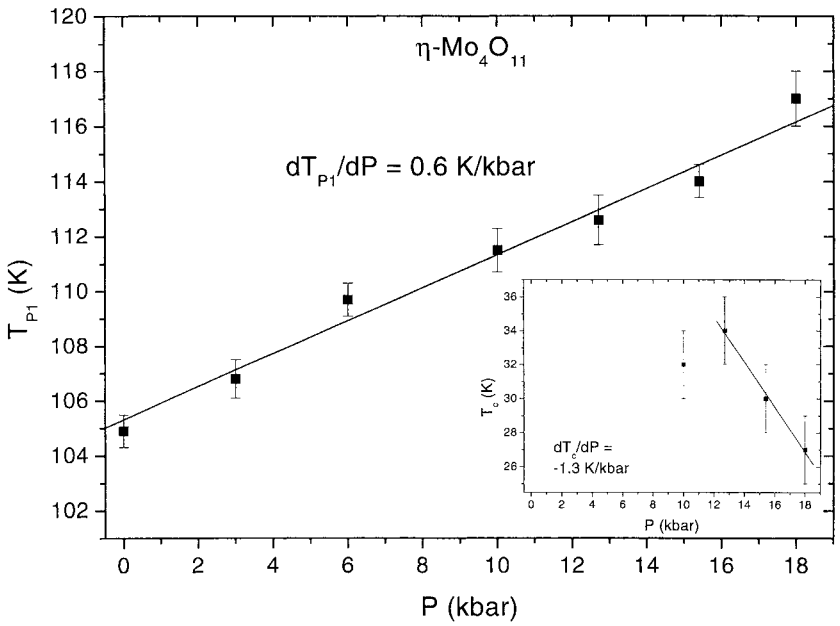

Figure 8. Transition temperature T_{p1} as a function of pressure for η-Mo_4O_{11}. The inset shows the transition temperature T_c as a function of pressure.

4. Discussion

We compare first the effect of a hydrostatic pressure on the Peierls transitions to similar studies on other CDW materials. In previous studies, it was shown that only in the oxide bronzes

$Na_{0.9}Mo_6O_{17}$ and $K_{0.9}Mo_6O_{17}$ (above 6 kbar) the Peierls transition temperature increases with pressure with large rates of the order of 5 K kbar^{-1}. Since the monophosphate bronzes and η-Mo_4O_{11} exhibit hidden one dimensionality, involving three quasi-1D Fermi surfaces, one may use, in an attempt to explain the results, the following mean field expression for the critical temperature valid in the 1D case and where the fluctuations are neglected:

$$k_B T_p = 2.28 E_F \exp\{-\eta\omega_0(2k_F)/\lambda^2 g(E_F)\}$$

where $\omega_0(2k_F)$ is the phonon frequency at the wavevector $2k_F$, $g(E_F)$ is the density of states at the Fermi level and λ^2 the corresponding electron–phonon coupling constant. It is generally believed that the lattice stiffens under pressure which increases the strain energy; $\omega_0(2k_F)$ is therefore expected to increase. This leads to a decrease of T_p with increasing pressure. The decrease of volume under pressure strengthens the interplane couplings and therefore the three dimensional character, reducing the nested portions of the Fermi surface. This leads to a decrease of $g(E_F)$ and therefore to a decrease of T_p. One should note that the rates dT_p/dP of decrease of T_p are comparatively larger than in several layered dichalcogenides [20]. This may be due to a larger compressibility in the case of the quasi-2D oxides.

The rates dT_{p1}/dP are negative and can be described in terms of lattice stiffening. They are approximately the same for $m = 4$ and $m = 5$ (see table 1). This suggests that the same type of chain of WO_6 octahedra is involved. This is consistent with the fact that the components along a^* and b^* of the wavevector q_1 of the corresponding modulation are nearly the same. Also, the rate dT_{p2}/dP for $m = 6$ is comparable to the rates dT_{p1}/dP observed in the $m = 4$ and $m = 5$ compounds. Again, the components of the wavevector q_2 ($m = 6$) are comparable to those of the above mentioned wavevector q_1 ($m = 4$, $m = 5$). Our results indicate that the slopes dT_{p1}/dP and dT_{p2}/dP are related to the nature of the WO_6 chains of octahedra.

For a given value of m ($m = 4$ or $m = 6$) one should note that the rate dT_p/dP is lower when the wavevector of the modulation has only one component along a^* (table 1). This may be related to an anisotropic compressibility of the system.

The Peierls transition temperature associated with a nesting vector along a^* is higher in $m = 6$ than in $m = 4$ (table 1). A better nesting along a^* than along $(a^* + b^*)$ may be responsible for the increase of the transition temperature and may be associated with the increase of thickness of the perovskite [WO_3]-type slabs when m increases.

The pressure dependence of T_{p2} in the $m = 4$ compounds is unusual and involves two competing mechanisms. At low pressure ($P < 5$ kbar), the increase of T_{p2} may result from an increase of the density of states $g(E_F)$ associated with an increase of hybridation of W(5d) and O(2p) orbitals, as expected if intraplane distances are shortened. Another possible mechanism is an increase of the transverse couplings, which reduces the one-dimensional fluctuations. For $m = 4$, there is an optimum value of the interchain couplings for the formation of a CDW. This optimum occurs for $P = 4$ kbar corresponding to the maximum of T_{p2}. At higher pressure, the conventional mechanism of lattice stiffening dominates.

The origin of the transition at $T_c = 30$ K in the $m = 5$ compound for which surprisingly dT_c/dP is positive (+0.3 K kbar^{-1}) is not yet elucidated. This transition is not accompanied by x-ray satellite peaks [12]. Moreover, a pronounced anomaly at 30 K in the resistivity measured in a large magnetic field is observed [13]. At low temperatures, electron correlations may play a role. They oppose to the formation of a CDW. Since the transfer integrals increase under pressure, a decrease of the electron–electron interactions is expected. This could lead to an increase of T_c with pressure. In this context, we suggest that T_c may correspond to the onset of a spin density wave state.

In η-Mo_4O_{11}, the rate of decrease of T_c above 13 kbar is less pronounced than in the bronzes. This may be related to a more rigid lattice or to different nesting conditions. The

intrinsic pressure dependence of T_c below 13 kbar is ambiguous because it may be hindered by the presence of the large temperature dependence of the resistivity below the transition at T_{p1}. Therefore no firm conclusion can be drawn for the rate of change of T_c under pressure below 13 kbar. The resistivity rise below T_c and above 13 kbar could be due to the generation of defects which would induce weak localization effects. The origin of the increase in T_{p1} is not yet explained. The associated wavevector of the modulation $q_1 = 0.23b^*$ plays a role similar to that observed in $m = 6$, $q_1 = 0.385a^*$. Although η-Mo_4O_{11} and the compound $m = 6$ have similar structures their nesting properties cannot be compared. The increase of T_{p1} could be due either to a decrease of electron–electron correlations or to better nesting properties under pressure.

5. Conclusion

In summary, we have observed large changes of the Peierls temperatures in the monophosphate tungsten bronzes. In the alternative compound with $m = 5$, the pressure dependence of T_c does not reflect the presence of the regular stacking of $m = 4$ and $m = 6$ layers. The rates of decrease of the transition temperatures with pressure are more pronounced when the corresponding wavevector of the modulation has components along $(a^* + b^*)$. The pressure dependences of T_{p1} and T_c in η-Mo_4O_{11} are different from that of the $m = 6$ compound although these oxides have similar structures. However, structural data under pressure would be necessary for a better interpretation of these properties.

Acknowledgments

The authors wish to thank G Fourcaudot for preparing η-Mo_4O_{11} crystals and M Greenblatt for helpful discussions.

References

[1] Greenblatt M (ed) 1993 Oxide bronzes *Int. J. Mod. Phys.* B **7** 4045
See also Schlenker C, Dumas J, Greenblatt M and van Smaalen S (eds) 1996 *Physics and Chemistry of Low Dimensional Inorganic Conductors (NATO-ASI Series B, 354)* (New York: Plenum)
[2] Schlenker C, Hess C, le Touze C and Dumas J 1996 *J. Physique* **6** 2061
Dumas J *et al* 1999 *J. Solid State Chem.* **147** 320
[3] Guyot H, Schlenker C, Pouget J P, Ayroles R and Roucau R 1985 *J. Phys. C: Solid State Phys.* **18** 4427
[4] Sorbier J P, Tortel H, Schlenker C and Guyot H 1995 *J. Physique* I **5** 221
[5] Ohara S, Koyano M, Negishi H, Sasaki M and Inoue M 1991 *Phys. Status Solidi* b **164** 243
[6] Inoue M, Ohara S, Horisaka S, Koyano M and Negishi H 1988 *Phys. Status Solidi* b **148** 659
[7] Whangbo M H, Canadell E, Foury P and Pouget J P 1991 *Science* **252** 96
Canadell E and Whangbo M 1990 *Phys. Rev.* B **43** 1894
Canadell E 1988 *Chem. Mater.* **10** 2770
[8] Teweldemedhin Z S, Ramanujachary K V and Greenblatt M 1989 *Phys. Rev.* B **46** 7897
[9] Wang E, Greenblatt M, Rachidi I E and Canadell E 1989 *Phys. Rev.* B **39** 12 969
[10] Foury P, Pouget J P, Wang E and Greenblatt M 1991 *Europhys. Lett.* **16** 485
[11] Roussel P, Foury P-Leylekian, Domengès B, Groult D, Labbé Ph and Pouget J P 1999 *Eur. Phys. J.* B **12** 497
[12] Foury P, Roussel P, Groult D and Pouget J P 1999 *Synth. Met.* **103** 2624
Foury P, private communication
[13] Beierlein U, Dumas J, Schlenker C, Groult D, Labbé Ph, Balthes E, Steep E and Bonfait G 1999 *J. Physique* IV **9** 375
[14] Hill S *et al* 1997 *Phys. Rev.* B **55** 2018
Sasaki M, Miyajima N, Negishi H, Negishi S, Inoue M, Kadomatsu H and Machel G 1999 *Solid State Commun.* **109** 357

[15] Beille J, Rötger A, Dumas J and Schlenker C 1991 *Phil. Mag. Lett.* **4** 221
Rötger A, Beille J, Laurant J M and Schlenker C 1993 *Solid State Commun.* **87** 913
[16] Fujishita H, Murayama C, Mori N and Sato M 1990 *J. Phys.: Condens. Matter* **2** 8751
[17] Escribe-Filippini C, Beille J, Boujida M, Marcus J and Schlenker C 1989 *Physica* C **162–164** 427
[18] Groult J P, Goreau M, Labbé Ph and Raveau B 1981 *Acta Crystallogr.* B **37** 2139
[19] Chaussy J, Haen P, Lasjaunias J C, Monceau P and Waysand G 1976 *Solid State Commun.* **20** 759
Nunez-Regueiro M, Mignot J M and Castello D 1992 *Europhys. Lett.* **18** 53
[20] Jérome D, Berthier C, Molinié P and Rouxel J 1976 *J. Physique* C **4** 124
Berthier C, Molinié P and Jérome D 1976 *Solid State Commun.* **18** 1393